

BOF ENDPOINT PREDICTION MODELING & RESULTS USING EFSOP[®] TECHNOLOGY AND A NOVEL IR SENSOR¹

Steven Gillgrass²
Salvador Rego-Barcena²
Omar Davis²
Vittorio Scipolo²
Joseph Maiolo²
Murray J. Thomson³

Abstract

Tenova Goodfellow Inc. has expanded the application of their Expert Furnace System Optimization Process (EFSOP[®]) to BOF steelmaking. The first EFSOP[®] system for the BOF has been installed on a 165-ton converter, with an open combustion fume system. A passive infrared sensor, sighted to measure the emissivity of the off-gas through the combustion gap of the BOF was tested. Initial results suggest that the sensor could be used to signal a transition in decarburization rate, near the end of the heat. The transition in the decarburization rate was signaled by a distinct peak in the particle emissivity. An advanced statistical methodology has been developed that predicts endpoint carbon from off-gas composition and process parameters. Evaluation of the EFSOP[®] Endpoint Predictor showed that carbon was detected within 1.15 points of carbon for > 90% of the heats, where the measured carbon was between 3.5 and 5.0 points. The EFSOP[®] Endpoint Predictor was also used to predict higher levels of carbon and was shown to be more accurate, as compared to other vessels in the shop. Benefit calculations support the expectation that accurate carbon prediction provides the steelmaker with increased productivity & yield, reduced cost, & a reduction in greenhouse gases. The off-gas composition has also been used to develop a dynamic state-space model of the BOF process. Model results for a representative heat are presented. The dynamic state-space model provides the basis for fine tuning of endpoint temperature and process analysis of the entire heat.

Keywords: Off-gas analysis; BOF steelmaking; Combustion processes; Energy efficiency; End-point detection; Slag detection

MODELAGEM DA PREDIÇÃO DO DESFECHO DE BOF E OS RESULTADOS USANDO TECNOLOGIA EFSOP[®] E UM MODERNO SENSOR IR

Resumo

Tenova Goodfellow Inc. expandiu a aplicação do seu Processo de Otimização do Sistema Especialista de Forno (EFSOP[®]) para fundição de aço BOF. O primeiro sistema EFSOP[®] para o BOF foi instalado em um conversor de 165 toneladas, com um sistema de combustão aberto com vapores. Um sensor infravermelho passivo, direcionado para medir a emissividade do efluente gasoso através do espaço de combustão do BOF que foi testado. Os resultados iniciais sugerem que o sensor pode ser usado para sinalizar uma transição na taxa de descarbonização, próximo do final da corrida. A transição na taxa de descarbonização foi sinalizada por um pico distinto na emissividade da partícula. Uma metodologia de estatística avançada foi desenvolvida que prevê o desfecho do carbono da composição de efluentes gasosos e parâmetros do processo. A avaliação do Preditor de Desfecho EFSOP[®] mostrou que o carbono foi detectado dentro de 1,15 pontos de carbono para > 90% das corridas, onde o carbono medido foi entre 3,5 e 5,0 pontos. O Preditor de Desfecho EFSOP[®] também foi usado para prever níveis mais elevados de carbono e demonstrou ser mais exato, em comparação a outros recipientes na fábrica. Cálculos benéficos confirmam a expectativa de que a previsão exata de carbono fornece ao operário siderúrgico o aumento da produtividade e lucro, custo reduzido e uma redução de gases de estufa. A composição de efluentes gasosos também foi usada para desenvolver um modelo dinâmico em espaço de estado do processo BOF. O resultado do modelo é apresentado por corrida representativa. O modelo dinâmico em espaço de estado fornece a base para o ajuste preciso da temperatura de desfecho e análise do processo de toda a corrida.

Palavras chave: Análise de gases de exaustão; Aciaria BOF; Processos de combustão; Eficiência energética.

¹ *Technical Contribution to the 40th Steelmaking Seminar – International, May, 24th-27th 2009, São Paulo, SP, Brazil.*

² *Tenova Goodfellow Inc., goodfellow@ca.tenovagroup.com*

³ *Department of Mechanical & Industrial Engineering, University of Toronto, Thomson@mie.utoronto.ca*

1 EFSOP[®] TECHNOLOGY FOR THE BOF

Tenova, comprised of a network of 30 operative companies located on five continents, is committed to the development of technology in the areas that greatly impact the future of the industries it serves. Energy efficiency, reduced operating costs, increased productivity, improving the environment and higher quality products are the drivers for Tenova innovation in the steel-industry.

Tenova Goodfellow's EFSOP[®] (Expert Furnace System Optimization Process) is a dynamic process control and optimization system that is based on the real-time measurement of off-gas composition. Though originally developed for steelmaking in the electric arc furnace (EAF),⁽¹⁻⁴⁾ the technology has been applied to oxygen steelmaking for endpoint control.^(5,6) This first EFSOP[®] system for the basic oxygen furnace (BOF) has been installed on a 165-ton vessel, used to convert a nominal mix of 120 tons of hot metal and 45 tons of scrap to steel for the automotive sector.

Figure 1 is a schematic of the EFSOP[®] system, as applied to the BOF. The system is comprised of:

- A patented water-cooled off-gas sampling probe, designed to withstand the steelmaking environment.
- The EFSOP[®] off-gas analyzer, for sample conditioning and analysis equipped with a customized purging system to keep the probe clear of dust and to eliminate plugging.
- Passive infrared gas sensors for off-gas temperature and particle emissivity measurements.
- A supervisory control and data acquisition (SCADA) system.

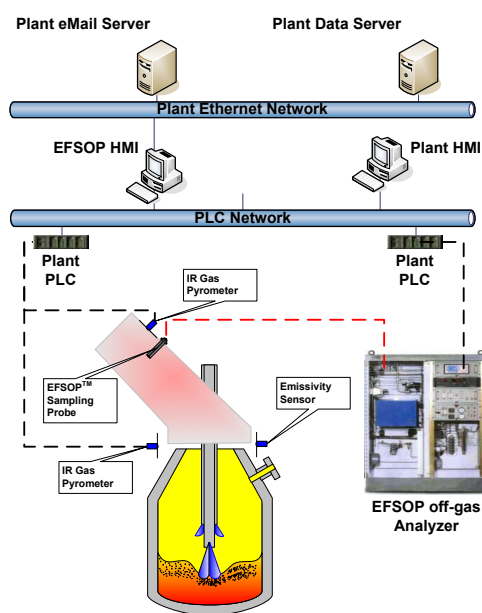


Figure 1: Schematic of the EFSOP[®] system applied to the BOF

The sampling probe is installed through a port in the panels of the BOF fume system. The probe is located downstream of the combustion gap to ensure that the sampled off-gases are completely mixed and combusted. The gases are drawn through a heated line to the EFSOP[®] analyzer, where they are analyzed, in real-time, for oxygen, carbon dioxide, carbon monoxide and hydrogen. Two infrared pyrometers (one located at the combustion gap and a second one at the downstream sampling location) are used to measure the temperature of the off-gas at the two locations. A third infrared sensor to

measure particle emissivity at the combustion gap was also tested. This first application of the EFSOP[®] analysis system for the BOF has proven to be highly reliable; with over 99% analysis uptime during the oxygen blow. To ensure a valid off-gas sample throughout the blowing period, the system is purged during natural breaks in the process (e.g. during tapping and between heats). This is sufficient to prevent plugging of sampling probe.

Composition measurements, as well as operational alarms and outputs from the analyzer are linked to the plant's PLC network. The EFSOP[®] SCADA (Supervisory Control and Data Acquisition) computer is linked to the same network and reads and logs off-gas data, as well as all relevant process data at a frequency of one second. Historical and real-time trends of the data are made available to the operator. Off-gas data, process data, and EFSOP[®] system alarms are emailed to Tenova Goodfellow's office in Mississauga, Canada, allowing process engineers to follow the operation remotely.

A plot of the measured off-gas composition profile for a representative heat is presented in Figure 2. The pattern displayed in the plot is typical and fairly consistent from one heat to the next. This particular plant operates with an open combustion system (not the more common suppressed combustion system found in most BOF shops); hence the high levels of oxygen and carbon dioxide indicated in the figure. Very little carbon monoxide is present indicating complete combustion of the off-gas with air entering the combustion gap. The large variations in the off-gas composition at the start of the heat are typical for this shop. The variation is due to the affect of additions (e.g. lime) added to the vessel at the start of the blow and pre-ignition conditions in the off-gas. After oxygen ignition at the start of the blow, the carbon dioxide ramps upwards as the lance is lowered and decarburization begins. The slight delay is attributed to the early oxidation of elements with a higher affinity for oxygen than carbon (e.g. Si, Mn). Near the conclusion of the blow, carbon dioxide falls rapidly as carbon is depleted. The pattern is mirrored in the concentration of oxygen.

It is well accepted that the kinetics of decarburization are driven by the rate of mass transfer of dissolved carbon to the reaction interface between liquid metal and iron oxide. At high carbon concentrations (approximately greater than 0.3% carbon), the mass transfer rate is sufficiently high that the rate of decarburization is controlled by the rate of oxygen supply to the steel bath. Below this concentration, the rate of decarburization is limited by the rate of carbon diffusion to the reaction interface.⁽⁷⁾ This mechanism is evident in the off-gas profile where carbon dioxide concentrations tend to remain fairly constant throughout the heat and to then decrease sharply as carbon is depleted near the end of the blow.

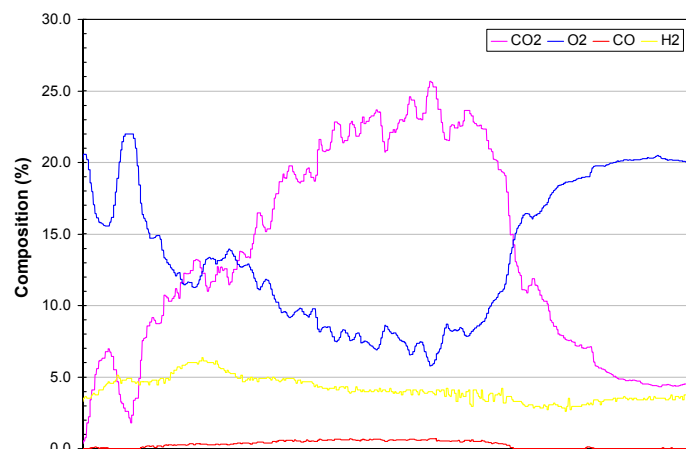


Figure 2: Measured Downstream Off-Gas Composition

2 PARTICLE EMISSIVITY AT THE COMBUSTION GAP AS A MARKER FOR DECARBURIZATION

As part of the SDTC project, Tenova Goodfellow Inc. collaborated with the Combustion Group at the University of Toronto, which had developed an optical sensor to measure particle emissivity and off-gas temperature in high temperature gas-particle streams. The sensor was mounted at the combustion gap of the BOF (Figure 1). The IR sensor and retrieval algorithms and a proof-of-concept test have been documented elsewhere.^(8,9) The measurement and methodology of the field trials were described previously.⁽¹⁰⁾ This section presents the process implications of the off-gas temperature and particle emissivity data when combined with the bath properties at first turndown.

The IR sensor consists of collection optics, a grating spectrometer and a 64-pixel pyroelectric array. It is calibrated to measure radiance [$W/m^2/\mu m/sr$] versus wavelength [μm] between 3.52 and 4.78 μm . The particle emissivity (ϵ_p) is spectral at $\lambda = 3.95 \mu m$, and therefore, is not the variable known as total emissivity. Apart from ϵ_p , the IR sensor also measures the temperature of the gas-particle stream (T_{g+p}) and the brightness temperature of the particles (T_p).

The process data for eight heats is shown in Table 1. The heats were grouped based on aim carbon content. Heats 1, 2, 6 and 7 had aim carbon levels greater than 0.30 and are labeled “high carbon heats”. The aim carbon for heats 3, 4, 5 and 8 was smaller than 0.08 and they are referred to as “low carbon heats”. Compositions are expressed in wt%.

Table 1: Aim, Turndown (TD1), Hot Metal (HM) and Initial (In) Process Data

Heat	Aim C	TD1 C	Aim T [°C]	HM T [°C]	TD1 T [°C]	Aim P	In P	TD1 P	P% Reduction
1	0.325	0.055	1582	1193	1691	0.015	0.049	0.009	81.6%
2	0.325	0.058	1582	1177	1667	0.015	0.051	0.004	92.2%
3	0.075	0.037	1607	1387	1726	0.070	0.045	0.007	84.4%
4	0.075	0.040	1599	1353	1706	0.070	0.042	0.005	88.1%
5	0.050	0.035	1610	1283	1669	0.015	0.041	0.007	82.9%
6	0.595	0.078	1555	1343	1717	0.015	0.048	0.019	60.4%
7	0.595	0.170	1555	1321	1705	0.015	0.045	0.019	57.8%
8	0.075	0.037	1607	1235	1733	0.070	0.048	0.005	89.6%

$$P\% \text{ Reduction} = (In P - TD1 P) / In P \%$$

Figure 3 shows the evolution of the two temperature variables (T_p (dotted line) and T_{g+p} (solid gray line)), and the particle emissivity (ϵ_p (solid black line)) from the IR sensor for the first two heats. To smooth out the original data, which was acquired every 2.025 s, Figure 3 uses a moving average every six data points. The moment at which the oxygen blow was stopped is marked by a solid vertical line. The time near the end of the oxygen blow when the particle emissivity peaked, and the particle temperature started to drop, is also identified by a thin, vertical line.

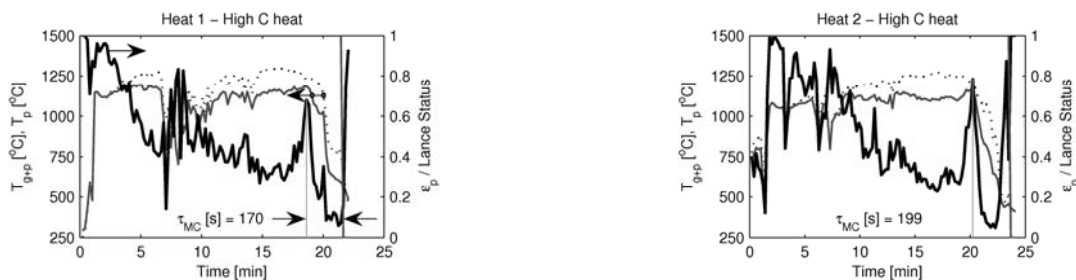


Figure 3: Temperature and Emissivity Measurements for Two Heats

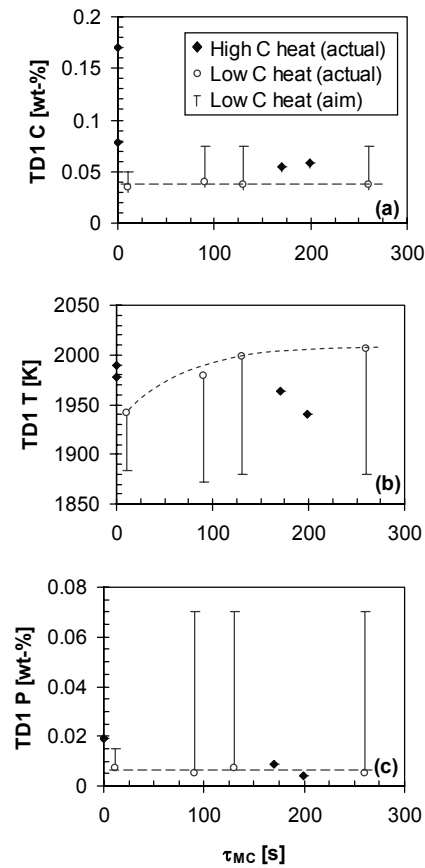


Figure 4: Correlation of minimum carbon time (τ_{MC}) and bath properties – (a) carbon, (b) temperature & (c) Phosphorus

The time elapsed between those two vertical lines is a new variable introduced here, which is called *minimum carbon time* (τ_{MC}) and is reported in seconds (Figure 3). This variable was set to zero when the oxygen lance went offline before ε_p peaked or T_p started to drop, which happened in heats 6 and 7, and was about to happen in heat 5 (the lowest τ_{MC} recorded, 11 s). The off-gas temperature also dropped before the oxygen injection stopped (heats 1-5, 8) but its decrease was less sharp than that of the particle brightness temperature. In terms of finding a suitable marker to signal operators of an important process change in the bath, the combination of a drop in T_p (instead of T_{g+p}) and the ε_p peak seems a reasonable choice. The name *minimum carbon* comes from the realization that when $\tau_{MC} > 0$, TD1 C had reached a bulk steady minimum value (between 0.035 and 0.058 wt-%) regardless of how long the oxygen blow was continued. When $\tau_{MC} = 0$, TD1 C was significantly higher, 0.078 in heat 6 and 0.170 in heat 7. Figure 4 shows the correlation of the newly defined variable (τ_{MC}) with the first turn down bath properties. The aim values for the four low carbon heats are also included. These plots will provide some insight into the final stage of the decarburization process.

The time at which the particle emissivity peaked (near the end of the heat) relative to the duration of the oxygen blow is shown in Table 2. Soon before this peak in emissivity, the operator should have seen an increase in the radiance of the flame. For heats with $\tau_{MC} > 0$ (1-5, 8), the particle emissivity peaked around 90% of the oxygen injection time and then decreased sharply (Table 2). This observation agrees well with Sharan's findings with a visible light sensor⁽¹¹⁾. It is after 80-90% of the total oxygen blown that the decarburization reaction between dissolved carbon in the liquid metal and gaseous oxygen goes from

being limited by the oxygen supply (gas diffusion control) to being limited by the carbon concentration in the liquid phase (mass transfer control)⁽⁷⁾. The transition in the decarburization mechanism is normally estimated to take place at carbon levels of 0.3%. At this point there is a sharp decrease in the evolution of CO, which lowers the off-gas emitted radiance. Carbon concentrations quickly stabilize around 0.04%⁽¹¹⁾ as can be observed in Figure 4a. Further oxygen injection also results in the (exothermic) oxidation of molten iron to form FeO, which travels to the slag layer while raising the bath temperature. This last feature, an increase in bath temperature with continued oxygen injection, is well exemplified by the low carbon heats in Figure 4b.

Table 2: ϵ_0 Peak Time as a Percentage of Total Oxygen Blow Time

Heat 1	Heat 2	Heat 3	Heat 4	Heat 5	Heat 6	Heat 7	Heat 8
87%	86%	90%	94%	99%	100%	100%	86%

The targets for carbon and temperature were achieved in all heats, even though Figure 4 shows only the aim values of the four low carbon heats. In order to reach their carbon target (see bars in Figure 4a), coke and other carbon-containing alloy additives such as manganese or chromium are introduced at tap. The phosphorus values were lower for the six heats with $\tau_{MC} > 0$, which met their target (Figure 11b). However in heats 6 and 7, $\tau_{MC} = 0$ and the first turndown phosphorus (0.019% in both cases) was higher than aim (0.015% for both). The desphosphorization reaction is very sensitive to the carbon content in the steel, and, as it has been shown, $\tau_{MC} = 0$ correlates with higher values of TD1 C. The average phosphorus reduction in the refined steel relative to the hot metal input for the two heats with $\tau_{MC} = 0$ was 59.1%, whereas for the other heats with $\tau_{MC} > 0$, the reduction was significantly higher (86.5%).

Finally, it is useful to know that the oxygen flow rate and lance height profiles (not shown here) were steady and very similar in the final minutes of all heats. This observation would reduce the likelihood of the possibility that the measured peak in the particle emissivity was caused by the operator's changes to the oxygen lance height towards the end of each heat.

It is because of the ability of τ_{MC} to correlate the endpoint properties of some heats that the time at which the particle emissivity peaks may be included as an input to the statistical model behind the EFSOP[®] Endpoint Predictor. The model already includes the time at which the last crossover between CO₂ and O₂ takes place (Figure 2). These findings are preliminary and further verification is required.

3 CARBON ENDPOINT DETECTION

BOF Operators rely on standardized practices and static charge models to achieve a desired endpoint hot metal chemistry (based on final grade specifications), at the lowest cost and highest productivity. Static charge models are mass and energy balances that take into account initial conditions and desired endpoint conditions, and calculate the expected total oxygen and fluxes that are required to reach that endpoint. The blow is stopped based on the pre-determined amount of oxygen or on other cues that help identify when the carbon has been depleted (e.g. color change of the flame, characteristic drop in the steam flow in the fume system cooling circuit).

In practice, static charge models are limited in their ability to predict endpoint because they do not take into account the dynamics of the process. Endpoint accuracy is also affected by uncertainties in the initial conditions (e.g. mass, temperature and composition of the hot metal; mass and type of scrap; mass of fluxes), by variations in the efficiency of the oxygen lance (within a heat; from heat-to-heat as the lance wears), and by changes to the geometry of the vessel with refractory wear. The operational limitations of endpoint

control, based on static charge models, are demonstrated in the following graphs (Figures 5 and 6).

Figure 5 is a histogram of the error in carbon endpoint (the difference between the aim carbon and the measured bath carbon using bomb Celox thermocouples). The error is reported in points of carbon (i.e. %C x 100). All heats stopped outside of 2% of total ordered (charge model) oxygen have been removed in order to determine the precision of the static charge model with respect to carbon endpoint. The data set was collected over a two-month period and is comprised of 900 heats. As indicated, the average error was found to be -0.12 points of carbon with a standard deviation of 2.43. The measured carbon at first sample was, on average lower than the aim, which is representative as this shop tends to overblow with respect to carbon.

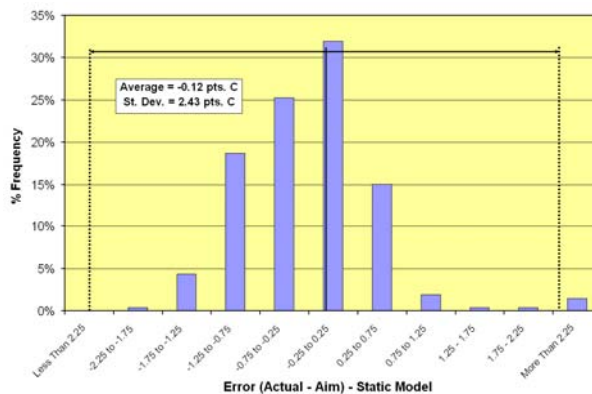


Figure 5: Error Distribution in Endpoint Carbon Using Static Charge Model

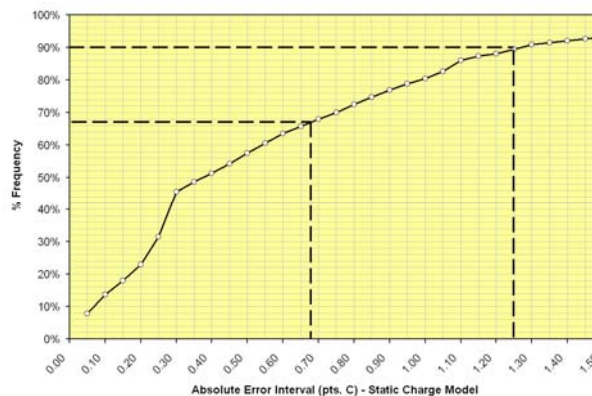


Figure 6: Cumulative Distribution of Carbon Error Using Static Charge Model

Figure 6 is a cumulative distribution plot of heats that fall within the error interval indicated. The error is determined as the absolute difference between the actual endpoint carbon and the measured carbon. The figure shows that the static charge model gives an accuracy of plus or minus 1.15 points of carbon for > 87% of heats and within 1.5 points of carbon for > 93% of heats. When considering both Figure 5 & 6, the current static charge model results in heats that are, on average, consuming more oxygen than required and achieving carbon aim at only a reasonable accuracy.

4 CARBON ENDPOINT DETECTION USING EFSOP®

EFSOP® endpoint detection uses real-time off-gas composition, along with measured process variables, to determine when the carbon endpoint has been reached. The EFSOP® Endpoint Predictor is comprised of two components:

1. Advanced multivariate statistical modeling
2. Dynamic state-space modeling

The statistical component of the EFSOP[®] Endpoint Predictor is based on analysis of actual process information (including off-gas chemistry) and endpoint results from over 300 heats. As with most statistical models, the EFSOP[®] Endpoint Predictor will be most accurate when applied in the range of data used to develop the model. This particular shop has > 97% of all endpoint aims between 4.0 and 4.5 points of carbon and > 92% of all endpoints less than 5.0 points of carbon.

The EFSOP[®] Endpoint Predictor, after being tuned and validated offline, was deployed and used predict endpoint in real-time. An evaluation has been conducted to determine the accuracy with which it was able to predict endpoint bath carbon in real-time. The evaluation period included over 500 heats and the results are presented in the following figures.

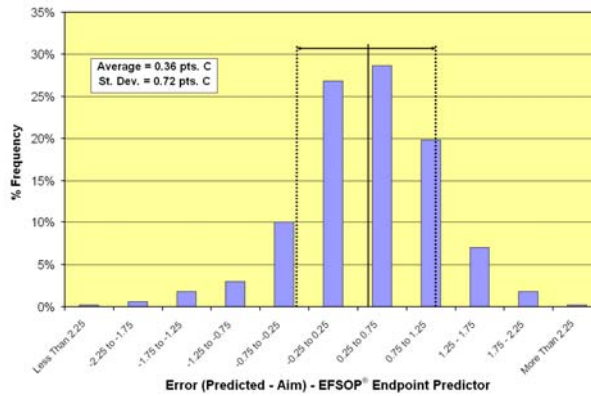


Figure 7: Error Distribution in Endpoint Carbon Using EFSOP[®] Endpoint Predictor

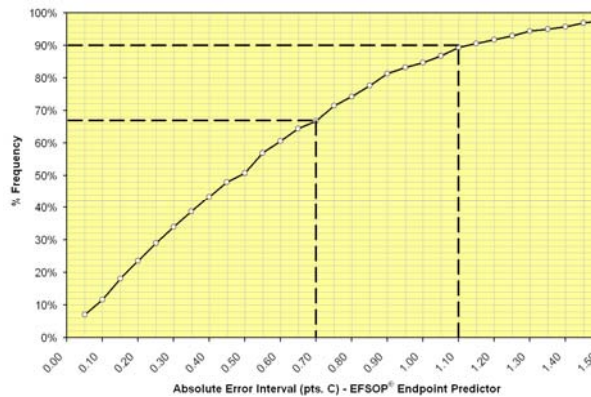


Figure 8: Cumulative Distribution of Absolute Carbon Error Using EFSOP[®] Endpoint Predictor

Figure 7 is a histogram of the error in carbon endpoint using the EFSOP[®] Endpoint Predictor. As indicated, the average error is 0.36 points of carbon with a standard deviation of 0.72. The EFSOP[®] predicted carbon was, on average higher than the aim, but within a much tighter standard deviation than heats using the static charge model. Figure 8 shows the cumulative distribution plot of heats as a function of the error interval. The figure shows that the statistical component of the EFSOP[®] Endpoint Predictor is able to predict within plus or minus 1.15 points of carbon for > 90% of heats and within 1.5 points of carbon for > 97% of heats. The error distribution and the cumulative distribution indicate that the EFSOP[®] Endpoint Predictor provides a significant improvement in endpoint control over the plant's operation with the static charge model.

Table 3: Process & Cost Benefits Using EFSOP® Endpoint Predictor

Items	Unit	% Change
Addition Carbon	lbs/heat	-2.7%
Aluminum Deoxidant	lbs/heat	-4.0%
Oxygen Consumption	lbs/heat	-0.7%
Ferrous alloys	lbs/heat	-1.6%
Heat Time	min/heat	-1.0%
Yield	%	0.3%

It is expected that more accurate endpoint control would result in lower oxygen consumption, lower ferroalloy and deoxidant consumption. At the conclusion of the EFSOP® Endpoint Predictor trial, these benefits to the plant were calculated and are presented in Table 3; where negative % change indicates a reduction. Other expected benefits include a reduction in refractory wear, quality and a reduction in end-point sampling consumables. These were not quantifiable during the course of the trial.

5 HIGHER CARBON DETECTION USING EFSOP®

During the trial period, there was an opportunity to test EFSOP® endpoint prediction on higher carbon endpoint. This particular plant has gotten away from a catch-carbon practice and tends to overblow with respect to carbon for higher carbon aims. Stopping the main oxygen blow at higher bath carbon composition results in numerous benefits including reduced alloy consumption (specifically manganese ferroalloys), reduced oxygen consumption and deoxidant consumption, increased yield and productivity. In the absence of sufficient process information to enrich the current statistical model, a combination of the dynamic off-gas data and the EFSOP® Endpoint Predictor were used to define an endpoint carbon aim of 0.100%. The scrap to hot metal ratio was modified based on the static charge to ensure that the temperature at the end of the oxygen blow would be acceptable given the reduction of chemical energy from the hot metal. Heats were run across all three BOF Vessels in the shop. The EFSOP® Endpoint Predictor was used to indicate the carbon endpoint on one of the vessels. The results of these trials were then compared to the endpoint results of the other vessels in the shop. The results are presented below in Table 4 and Figure 9.

Table 4: Results for 0.100% carbon aims using EFSOP® Endpoint Predictor

BOF Vessel	# of Heats	Average C %	Standard Deviation C (%)	Average Absolute C Error (%)
Non-EFSOP®	53	0.1083	0.0589	0.0406
EFSOP® Controlled	16	0.0924	0.0248	0.0222

On average, the Non-EFSOP® vessels performed fairly well, achieving the aim of 0.100% C at endpoint. However, a detailed statistical analysis shows a very large variation for the endpoint bath carbon across those vessels. As well, there were two reblows specifically due to carbon on the non-EFSOP® vessels and an overall reblow rate of 9.43%. The vessel using the EFSOP® Endpoint Predictor also achieved the aim of 0.100% C +/- 0.01%, but there was significantly less variation compared to the Non-EFSOP® vessels; no reblows due to carbon and an overall reblow rate of 6.25%.

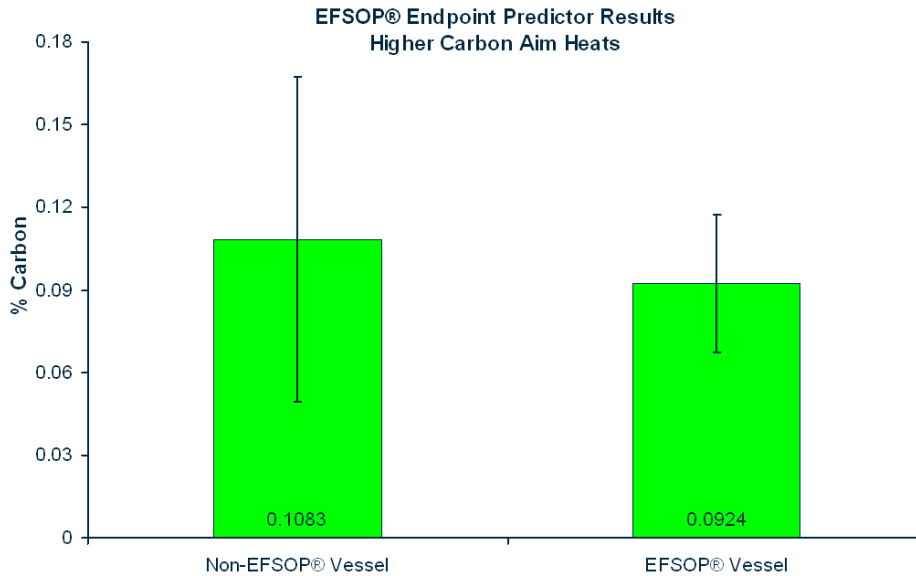


Figure 9: Results for Higher Carbon Aims Using EFSOP® Endpoint Predictor

6 DYNAMIC STATE-SPACE MODELING

Whereas the statistical approach for carbon endpoint prediction has produced favorable results, endpoint temperature prediction has proved more challenging. Working under the assumption that a better approach to predicting temperature endpoint would be to use a core mechanistic model that would be fine-tuned using multivariate statistical methods, a rigorous, state-space model of the Basic Oxygen Furnace has been developed. The EFSOP® dynamic model component, unlike the static charge model approach where only initial and final conditions are taken into account, makes use of real-time off-gas composition to calculate the mass and energy balance over the entire course of the blow. The general details of the EFSOP® approach have been reported earlier⁽⁶⁾.

The advantage of using EFSOP® is that the off-gas information provides a dynamic measure of oxygen utilization over the course of the heat and allows a real-time evaluation of the actual efficiency of the oxygen imparted to the process for both bath refining and post combustion. Variability in the efficiency with which oxygen is delivered to the bath is not unexpected and is affected by many influences, such as: lance wear, variations in lance height, variations in the oxygen flow rate, refractory wear, etc.

The model is comprehensive in that it takes as its inputs the real-time off-gas composition and oxygen rate and calculates the efficiency of the oxygen delivery system. The model provides an indication of the partition of oxygen between post-combustion (combustion of carbon monoxide to carbon dioxide), decarburization reactions and oxidation reactions. Another component of the dynamic model is a module that calculates the rate of melting of fluxes and scrap and the associated energy balances. These are in turn used to dynamically calculate the properties of the bath and slag over the course of the heat.

The greatest challenge encountered in the development of the dynamic model has been tuning the model to the process. The accuracy in the initial conditions (i.e. mass and composition of scrap and hot metal) as well as the accuracy in the measured final bath conditions (i.e. endpoint carbon and temperature; slag analysis) greatly influence the predictive ability of the model. Uncertainties in the precision of the input data in industry are common issues, however it is expected that this could be effectively dealt with using multivariate statistical methods. This effort is ongoing, however some preliminary results are presented below in Figures 10 and 11.

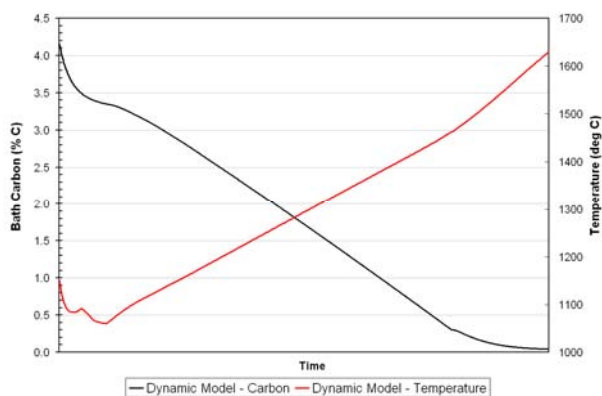


Figure 10: Dynamic Model Results for an Entire Heat

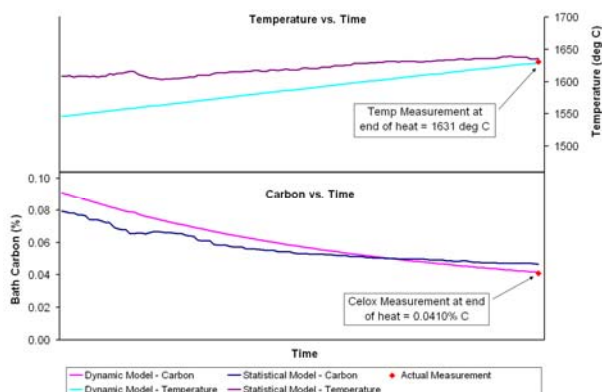


Figure 11: Comparison of Dynamic Model Results with Statistical Model & Actual

Figure 10 is an example of the carbon and temperature profiles calculated from the real-time process data and off-gas information for the entire oxygen blow. The general trend of the bath carbon provided by the model is as expected. Of particular importance is the inflexion point in the carbon trend where the dynamics move from mixing to diffusion controlled. Figure 11 presents an enlarged view of the end of the blow and shows a comparison of dynamic model results and the actual carbon and temperature endpoints measured at the end of this particular heat. The results of the statistical model are also shown for comparison. As shown in the graph, both endpoint carbon and temperature for the dynamic model compare very well with the measured endpoint and the statistical model endpoint.

7 CONCLUSIONS AND FUTURE WORK

Online evaluation of the EFSOP[®] approach to endpoint prediction showed that carbon endpoint can be identified with greater accuracy and frequency than is possible with the plant's current static charge model approach. The EFSOP[®] endpoint predictor is able to predict carbon within 1.15 points of the measured value for > 90% of the heats and within 1.50 points of the measured value for > 97% of the heats. Based on these results and measured benefits, the plant has adopted the EFSOP[®] Endpoint Predictor for use on the BOF for 100% of their heats.

The EFSOP[®] Endpoint Predictor was also used to facilitate the production of grades with higher carbon aims. The EFSOP[®] approach yielded increased accuracy and a lower standard deviation, compared to other vessels in the shop. The ability to move towards a "catch-carbon" practice will provide additional savings and benefits above current measured values.

A distinct peak in particle emissivity measured at the combustion gap signals a transition in decarburization. It may be possible to use the time at which the peak occurs to improve the accuracy of the EFSOP[®] Endpoint Predictor.

A dynamic model of the BOF process, based on real-time off-gas measurements, has been developed. The model has been tested online, using real-time process and off-gas data. Early indications are that it performs well, however a greater number of heats are required for validation. Ultimately, TGI intends to use the model as a “soft-sensor” to supplement the multivariate approach for temperature end-point prediction.

Acknowledgements

The authors of this paper would like to thank Sustainable Development Technology Canada (SDTC) for providing partial funding for this 3-year project. SDTC is a not-for-profit Canadian foundation that finances and supports the development and demonstration of clean technologies to provide solutions to issues of climate change, energy efficiency and reduced greenhouse gas emissions.

REFERENCES

- 1 MAIOLO, J.; EVENSON, E.J.; NEGRU, O.I. Goodfellow EFSOP[®] Successes at TAMSA, Veracruz. *AISTech 2004*, Nashville, TN, Sept 2004.
- 2 KELLEHER, J., KHAN, M.I. Yield and Productivity Savings Using Goodfellow EFSOP[®] at MacSteel Arkansas. *AISTech 2006*, Cleveland, OH, May 2006.
- 3 VENSEL, D., KHAN, M.I. EAF Performance Improvement at Nucor Steel Auburn using Goodfellow EFSOP[®]. *AISTech 2006*, Cleveland, OH, May 2006.
- 4 MAIOLO, J.A., BOUTAZAKHTI, M., LI, C.W., WILLIAMS, C., Developments towards an Intelligent Electric Arc Furnace at CMC Texas using Goodfellow EFSOP[®] Technology. *AISTech 2007*, Indianapolis, IN, May 7-10, 2007.
- 5 MAIOLO, J., ZULIANI, D., BOF End-Point Prediction using EFSOP[®] Technology. *Metal Producing & Processing*, Nov/Dec 2008, Vol.46, No.6, pp.15-18.
- 6 SCIPOLO, V., MAIOLO, J., LI, C.W., GOLDBERG, B., ZULIANI, D. Application of EFSOP Holistic Optimization[®] Technology to Oxygen Steelmaking. *AISTech 2007*, Pittsburgh, PA, May 5-8, 2008.
- 7 TURKDOGAN, E.T., FREUHAN, R.J. Fundamentals of Iron and Steelmaking, *The Making, Shaping and Treating of Steel 11th Edition*, The AISE Steel Foundation., Pittsburgh, PA, 1998, pp.123-126.
- 8 REGO-BARCENA, S., SAARI, R., MANI, R., EL-BATROUKH, S., THOMSON, M.J. Real time, non-intrusive measurement of particle emissivity and gas temperature in coal-fired power plants”, *Meas. Sci. Technol.*, 2007, Vol.18, pp.3479-3488.
- 9 REGO-BARCENA, S., THOMSON, M.J. Particle effects on the emissivity and temperature of optically-thick, mixed media retrieved by mid-IR emission spectroscopy. *J. Quant. Spectrosc. Rad. Transfer*, 2007, Vol.109, pp.1325-1334.
- 10 REGO-BARCENA, S., MANI, R., YANG, F., SAARI, R., THOMSON, M.J. Real time, optical measurement of gas temperature and particle emissivity in a full-scale steelmaking furnace. *Metall. Mater. Trans. B*, accepted Oct 2008.
- 11 SHARAN, A. Light sensors for BOF carbon control in low carbon heats. *Steelmaking Conf. Proc. Iron & Steel Society*, Toronto, ON, 1998.